Inorg. Chem. **2003**, *42*, 1070–1075

Coordination of BF_4^- to Oxovanadium(V) Complexes, Evidenced by the Redox Potential of Oxovanadium(IV/V) Couples in CH_2Cl_2

Kenichi Oyaizu, Eniya Listiani Dewi, and Eishun Tsuchida*

Advanced Research Institute for Science and Engineering, Waseda University, Tokyo 169-8555, Japan

Received October 3, 2002

The oxidation of oxovanadium(IV) complexes [$LV^{IV}O$] (L = tetradentate Schiff-base ligands such as *N,N′*-ethylenebis(salicylideneaminate)(2–) (salen) and *N,N′*-2,2-dimethylpropylenebis(salicylideneaminate)(2–) (salpn)) to [$LV^{V}O]^+$, believed to be responsible for the voltammetric response near 0.6 V vs Ag/AgCl in CH_2Cl_2 in the presence of tetrabutylammonium tetrafluoroborate as a supporting electrolyte, is in fact coupled to a homogeneous process where $[LVO]^+$ coordinates BF_4^- to form a neutral complex formulated as [$LVOBF_4$]. The formation constants for [$VO(salen)BF_4$] and [$VO(salpn)BF_4$] are evaluated to be $K_{salen}^{-1} = 1.1 \times 10^2$ M^{-1} and $K_{salpn}^{-1} = 1.4 \times 10$ M^{-1}, respectively. Crystal structure of [$VO(salen)BF_4$] reveals that one of the fluorine atoms in BF_4^- is so close to the vanadium(V) atom as to be practically bound in the solid state.

Introduction

Cyclic voltammetry of (*N,N′*-ethylenebis(salicylideneaminato))oxovanadium(IV) ([$V^{IV}O$(salen)]) in polar solvents such as CH_3CN,[1,2] CH_3OH,[2] DMF,[2,3] and DMSO[4] in the presence of supporting electrolytes shows a reversible oxidation−reduction couple ranging in potentials from +0.29 to +0.46 V vs SCE depending on the solvent, which has been ascribed to a simple electrode reaction, [$V^{IV}O$(salen)] $\rightleftarrows$ $[V^{V}O(salen)]^+ + e^-$. In a less donating solvent CH_2Cl_2, the voltammetric response is more complex: with tetraethylammonium perchlorate ([NEt_4][ClO_4])[4] or tetrabutylammonium tetrafluoroborate ([NBu_4][BF_4])[5] as the supporting electrolyte, a single oxidation−reduction couple is observed at much higher potentials (near 0.64 V vs SCE) than in polar solvents, while it splits into two reversible couples separated by ca. 0.1 V by the replacement of the supporting electrolyte with [NBu_4][PF_6] and at high concentrations of [VO(salen)] (>1 mM).[6,7] These redox responses could be rationalized by considering the preference of vanadium(V) to be six-coordinate rather than five[6,8−10] that may drive the coordination of additional ligands such as polar solvent molecules and electrolyte anions in the axial site on the unoccupied side of $[VO(salen)]^+$, or, in the absence of these external ligands, the association of mononuclear species to form dinuclear VOVO[6] (or higher oligomerized[7]) units.

In this report, we describe that the oxidation of [VO(salen)] to $[VO(salen)]^+$, believed to be responsible for the voltammetric wave in CH_2Cl_2 in the presence of [NBu_4][BF_4], is in fact coupled to a homogeneous process in which $[VO(salen)]^+$ coordinates BF_4^- to form a neutral complex formulated as [$VO(salen)BF_4$]. The crystal structure of [$VO(salen)BF_4$] reveals that one of the fluorine atoms in BF_4^- and the vanadium(V) atom are so closely spaced as to be practically bound in the solid state. The formation constant of [$VO(salen)BF_4$] in CH_2Cl_2 and the oxidation potential of [VO(salen)] unperturbed by any coupled reaction are evalu-

* Author to whom correspondence should be addressed. E-mail: eishun@mn.waseda.ac.jp.

(1) (a) Liu, Z.; Anson, F. C. *Inorg. Chem.* **2000**, *39*, 274, 1048. (b) Bonadies, J. A.; Butler, W. M.; Pecoraro, V. L.; Carrano, C. J. *Inorg. Chem.* **1987**, *26*, 1218.
(2) Bonadies, J. A.; Carrano, C. J. *J. Am. Chem. Soc.* **1986**, *108*, 4088.
(3) Kapturkiewicz, A. *Inorg. Chim. Acta* **1981**, *53*, L77.
(4) Seangprasertkij, R.; Riechel, T. L. *Inorg. Chem.* **1986**, *25*, 3121.
(5) Tsuchida, E.; Oyaizu, K.; Dewi, E. L.; Imai, T.; Anson, F. C. *Inorg. Chem.* **1999**, *38*, 3704.
(6) Choudhary, N. F.; Connelly, N. G.; Hitchcock, P. B.; Leigh, G. J. *J. Chem. Soc., Dalton Trans.* **1999**, 4437.
(7) Liu, Z.; Anson, F. C. *Inorg. Chem.* **2001**, *40*, 1329.
(8) (a) Yamamoto, K.; Oyaizu, K.; Tsuchida, E. *J. Am. Chem. Soc.* **1996**, *118*, 12665. (b) Oyaizu, K.; Yamamoto, K.; Yoneda, K.; Tsuchida, E. *Inorg. Chem.* **1996**, *35*, 6634.
(9) (a) Carrano, C. J.; Mohan, M.; Holmes, S. M.; de la Rosa, R.; Butler, A.; Charnock, J. M.; Garner, C. D. *Inorg. Chem.* **1994**, *33*, 646. (b) Riley, P. E.; Pecoraro, V. L.; Carrano, C. J.; Bonadies, J. A.; Raymond, K. N. *Inorg. Chem.* **1986**, *25*, 154.
(10) (a) Fairhurst, S. A.; Hughes, D. L.; Leigh, G. J.; Sanders, J. R.; Weisner, J. *J. Chem. Soc., Dalton Trans.* **1994**, 2591. (b) Hughes, D. L.; Kleinkes, U.; Leigh, G. J.; Maiwald, M.; Sanders, J. R.; Sudbrake, C.; Weisner, J. *J. Chem. Soc., Dalton Trans.* **1993**, 3093. (c) Hills, A.; Hughes, D. L.; Leigh, G. J.; Sanders, J. R. *J. Chem. Soc., Dalton Trans.* **1991**, 61.

10.1021/ic0205987 CCC: $25.00
Published on Web 01/21/2003

ated electrochemically and compared to those of oxovanadium complexes with salpn ligands (salpn = *N*,*N*′-2,2-dimethylpropylenebis(salicylideneaminate)(2−)). To simplify the system, the solutions of oxovanadium(IV) complexes are kept so dilute (0.1 mM) throughout this work that one need not take the VOVO formation[6,7] into account.

Experimental Section

Materials. [VO(salen)],[2] [VO(salen)BF_4],[11] [VO(salpn)],[12] and [VO(salpn)$NCCH_3$][BF_4][12] were prepared as previously reported and purified by recrystallization from CH_2Cl_2−CH_3OH or CH_3CN. Decamethylferrocene (DMFc) was obtained from Kanto Chem. Co. and used without purification. Tetrabutylammonium tetrafluoroborate ([NBu_4][BF_4]) was obtained from Tokyo Kasei Co. and purified by recrystallization from benzene−ethyl acetate in a volume ratio of 2:1. Tetrabutylammonium perchlorate ([NBu_4][ClO_4]) and tetrabutylammonium hexafluorophosphate ([NBu_4][PF_6]) of electrochemical grades were obtained from Tokyo Kasei Co. and used as received. Dichloromethane was purified by distillation over P_2O_5.

Apparatus and Procedures. Electrochemical measurements were carried out in a conventional one-compartment cell using a Bioanalytical Systems model 100B/W electrochemical analyzer. A 1.6 mm diameter platinum disk electrode ($A = 2.0 \times 10^{-2}$ cm^2) and a 10 μm diameter platinum microelectrode ($A = 7.9 \times 10^{-7}$ cm^2) were used as the working electrode in voltammeric experiments. Prior to use the disk electrode was polished with a 0.3 μm alumina paste and rinsed with water, acetone, and distilled CH_2Cl_2. The microelectrode was rinsed with acetone and distilled CH_2Cl_2 without polishing. The auxiliary electrode was a platinum wire. The reference electrode was Ag/AgCl in CH_2Cl_2 containing 0.1 M [NBu_4][ClO_4]. All potentials are quoted with respect to this electrode except where noted. ^{19}F NMR spectra were obtained on JEOL EX-270 using CF_3COOH as an external standard at $\delta = -77.00$ ppm.

X-ray Crystallography. Black cubic crystals of [VO(salen)BF_4] and black prismatic crystals of [VO(salpn)$NCCH_3$][BF_4] were grown from CH_3CN solutions after layering with diethyl ether. All measurements were performed on a Rigaku AFC5R diffractometer with graphite monochromated Cu Kα radiation and a 12 kW rotating anode generator for [VO(salen)BF_4] and with Mo Kα radiation and a 6 kW rotating anode generator for [VO(salpn)$NCCH_3$][BF_4]. The structures were solved by heavy-atom Patterson methods and expanded using Fourier techniques. In [VO(salen)BF_4], the non-hydrogen atoms were refined anisotropically. In [VO(salpn)$NCCH_3$][BF_4], the B and F atoms were refined isotropically while the rest of non-hydrogen atoms were refined anisotropically. In the refinement of both molecules, hydrogen atoms were included but not refined. The final cycle of the full-matrix least-squares refinement[13] was based on the observed reflections ($I > 3\sigma(I)$) and converged with unweighted and weighted agreement factors of $R = \sum||F_o| - |F_c||/\sum|F_o|$ and $R_w = (\sum w(|F_o| - |F_c|)^2/\sum wF_o^2)^{1/2}$. All calculations were performed using the teXsan crystallographic software package from Molecular Structure Corporation.[14]

Data for [VO(salen)BF_4]: monoclinic, space group *C*2/c (#15), $a = 15.449(11)$ Å, $b = 8.370(3)$ Å, $c = 26.036(11)$ Å, $\beta = 91.08(5)°$, $V = 3366(3)$ Å^3, $Z = 8$, final $R = 0.065$, $R_w = 0.045$.

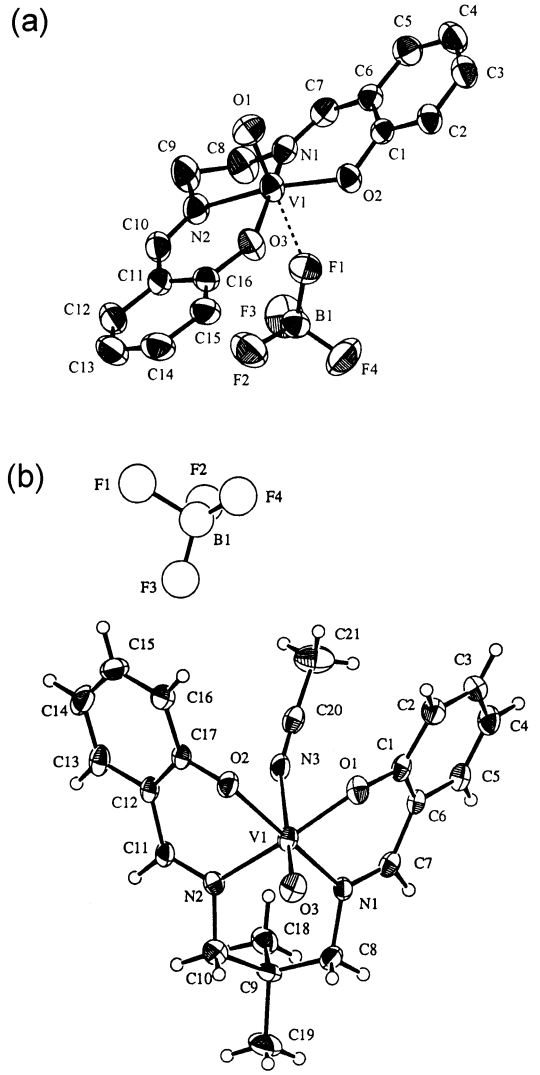

Figure 1. ORTEP view of (a) [VO(salen)BF_4] (50% probability ellipsoids) and (b) [VO(salpn)$NCCH_3$][BF_4] (30% probability ellipsoids). Hydrogen atoms in [VO(salen)BF_4] are omitted for clarity. Selected atom distances (Å) for (a): V(1)−O(1), 1.577(2); V(1)−F(1), 2.380(2); B(1)−F(1), 1.409(4); B(1)−F(2), 1.365(4); B(1)−F(3), 1.375(4); B(1)−F(4), 1.359(4). Data for (b): V(1)−O(3), 1.582(5); V(1)−N(3), 2.508(7).

Data for [VO(salpn)$NCCH_3$][BF_4]: orthorhombic, space group *P*bca (#61), $a = 20.19(2)$ Å, $b = 17.43(2)$ Å, $c = 12.97(2)$ Å, $V = 4564(14)$ Å^3, $Z = 8$, final $R = 0.073$, $R_w = 0.088$.

Results and Discussion

Figure 1a shows the crystal structure of [VO(salen)BF_4] in which the vanadium(V) atom extends 0.319 Å above the best N_2O_2 least-squares plane of the salen ligand with a very short distance to the BF_4^- fluorine (2.380(1) Å). A comparison with the structure of [VO(salen)][ClO_4][1b] suggests that, since the BF_4^- anion is a stronger base[1a] and hence more coordinating than ClO_4^- (V−O distance = 2.456(3) Å), the atomic arrangement in [VO(salen)BF_4] more closely represents a six-coordinate vanadium(V) atom. The formation of the V(1)−F(1) bond represented by the dashed line in Figure 1a is reflected in the significant elongation of the B(1)−F(1) bond compared to the other B−F bonds. On the other hand, [VO(salpn)$NCCH_3$][BF_4] crystallized as the external axial ligand for CH_3CN instead of BF_4^- (Figure 1b).

(11) Tsuchida, E.; Yamamoto, K.; Oyaizu, K.; Iwasaki, N.; Anson, F. C. *Inorg. Chem.* **1994**, *33*, 1056.
(12) Fairhurst, S. A.; Hughes, D. L.; Kleinkes, U.; Leigh, G. J.; Sanders, J. R.; Weisner, J. *J. Chem. Soc., Dalton Trans.* **1995**, 321.
(13) Least-squares, function minimized: $\sum w(|F_o| - |F_c|)^2$, where $w = (\sum(F_o)^2 + (p^2(F_o)^2/4))^{-1}$.
(14) teXsan: Crystal Structure Analysis Package, Molecular Structure Corporation, 1985 and 1992.

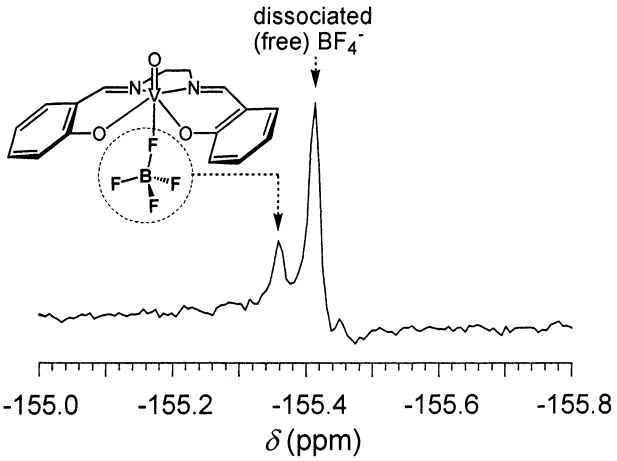

Figure 2. 270 MHz ^{19}F NMR spectrum of a solution of 2.0 mM [VO(salen)BF_4] in CD_2Cl_2. Trifluoroacetic acid ($\delta = -77.00$ ppm) was used as the external standard.

The dissociation of BF_4^- from the $[VO(salpn)NCCH_3]^+$ cation is indicated by the significant displacement of BF_4^- in the crystal lattice which prevents the anisotropic refinement. A comparison of the two structures may indicate that the coordination of BF_4^- to the "umbrella-shaped"[12] $[VO(salpn)]^+$ cation is less favorable than to the sterically less crowded $[VO(salen)]^+$ cation.

Figure 2 shows the ^{19}F NMR spectrum of a solution of $[V^VO(salen)BF_4]$ in which a high resolution is accomplished using the ^{2}D resonance of CD_2Cl_2. In addition to the singlet peak at $\delta = -155.41$ ppm due to the resonance of dissociated (free) BF_4^- anion,[15] a unimodal peak is observed at the lower field ($\delta = -155.36$ ppm) which can be ascribed to the resonance of the BF_4^- anion coordinated to the oxovanadium(V) center. A rough diagnosis of the coordination kinetics is provided by the peak shapes. The two-peak profile demonstrates that the BF_4^- anion coordinates to and dissociates from the oxovanadium(V) center so slowly that the equilibrium is frozen during the time it takes for the fluorine atoms to undergo resonance. However, the unimodal peak shape for the coordinated BF_4^- anion indicates that the inequivalent fluorine resonances are coalesced, probably due to the rapid rearrangement within the coordination sphere of the oxovanadium(V) center. The peak intensity for the free BF_4^- anion relative to that for the coordinated BF_4^- anion (5.2 for a solution prepared by dissolving 2.0 mM $[V^VO(salen)BF_4]$ at 25 °C) gives an estimation for the concentrations of the BF_4^- anions in the solution coordinated to or dissociated from the oxovanadium(V) center and thus for the dissociation equilibrium constant ($K_{salen} = 8.8 \times 10^{-3}$ M) which is in good agreement with that evaluated electrochemically (vide infra). The peak due to the coordinated BF_4^- anion becomes less prominent at higher temperatures because of the larger extent of the dissociation of BF_4^-, while it broadens at lower temperatures as a result of the slower inner-sphere rearrangement.

Figure 3a shows cyclic voltammograms for solutions of 0.1 mM [VO(salen)] in CH_2Cl_2 in the presence of $[NBu_4][PF_6]$ and 0.1 mM DMFc. Each voltammogram shows two distinct waves at different potentials. The oxidation−reduction couple near 0.6 V is assignable to the oxovanadium(IV/V) couple and is not split into multiple peaks. The oxidation−reduction couple near −0.1 V is assignable to the $DMFc^{0/+}$ couple. These two couples are so separated in potentials that one need not take the cross redox reaction between $[VO(salen)]^{0/+}$ and $DMFc^{0/+}$ couples into account. Both waves show characteristics of a reversible one-electron transfer, i.e., $i_{pa}/v^{1/2}$ and E_{pa} independent of scan rate, the peak-to-peak separation ΔE_p ($=E_{pa} - E_{pc}$) in the range of $59 < \Delta E_p \leq 84$ mV, and $i_{pa}/i_{pc} \approx 1$ (where i_{pa} and i_{pc} are the

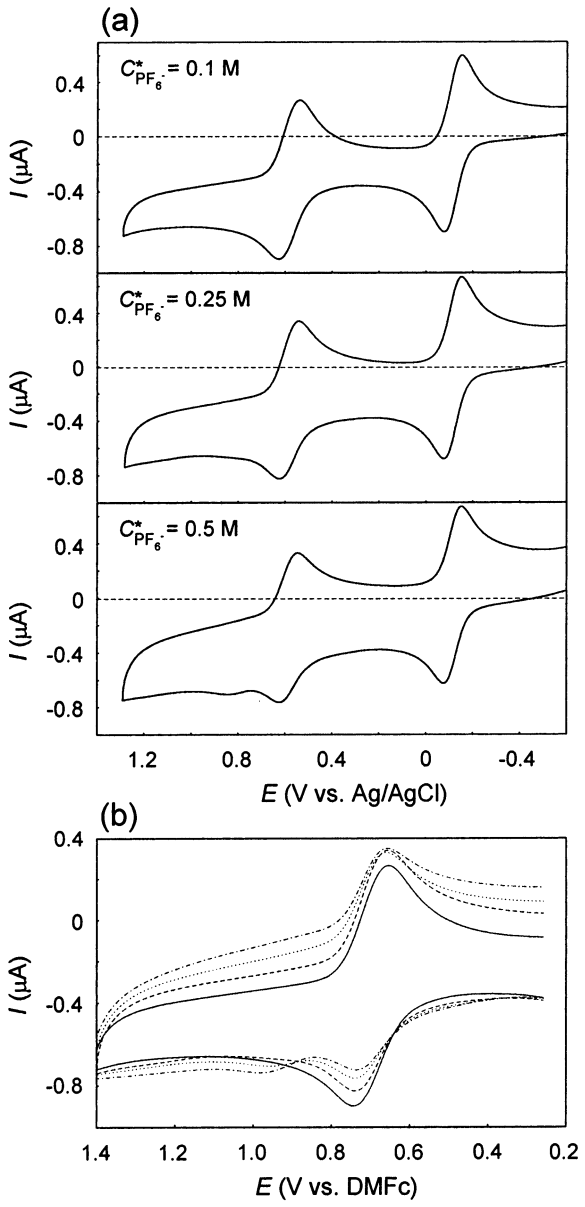

Figure 3. (a) Cyclic voltammetry of a 0.1 mM solution of [VO(salen)] in CH_2Cl_2, also containing 0.1 mM DMFc and a supporting electrolyte recorded with a platinum disk electrode (2.0×10^{-2} cm^{-2}) scanned at $v = 100$ mV s^{-1}. Supporting electrolyte ($[NBu_4][PF_6]$): $C^*_{PF_6^-} = 0.1$, 0.25, and 0.5 M as shown in the figure. The position of zero current is shown by the dashed line. (b) Cyclic voltammograms obtained with $C^*_{PF_6^-} = 0.1$ (—), 0.25 (− − −), 0.5 (· · ·), and 0.75 M (— · —) superimposed upon each other. The average of anodic and cathodic peak potentials (($E_{pa} + E_{pc}$)/2) for DMFc was set at 0 V in each voltammogram.

(15) (a) Brownstein, S.; Latremouille, G. *Can. J. Chem.* **1978**, *56*, 2764. (b) Hartman, J. S.; Schrobilgen, G. J. *Inorg. Chem.* **1972**, *11*, 940.

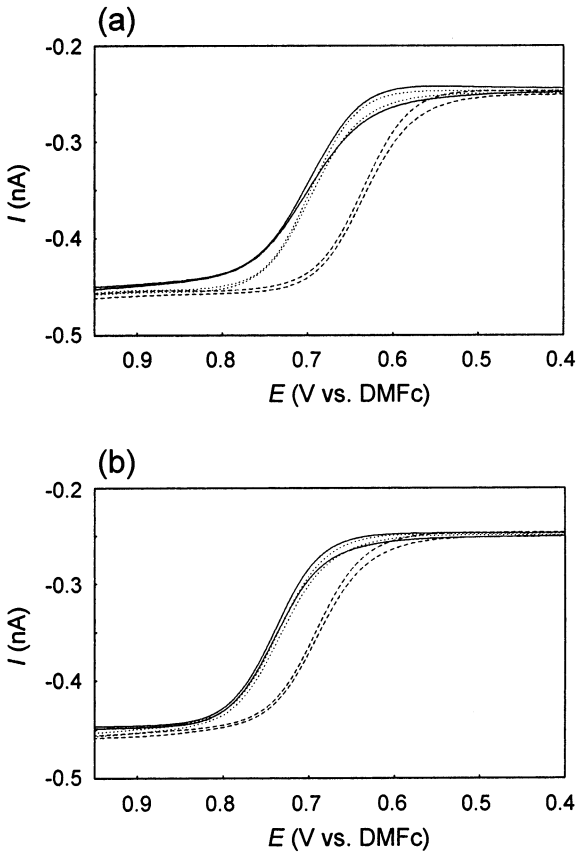

Figure 4. (a) Cyclic voltammetry of a 0.1 mM solution of [VO(salen)] in CH_2Cl_2 recorded with a platinum microelectrode (7.9×10^{-7} cm^2) scanned at 25 mV s^{-1}. Supporting electrolyte ([NBu_4][X]): $C^*_{X^-} = 0$ M (—), $C^*_{BF_4^-} = 0.1$ M (– – –), $C^*_{PF_6^-} = 0.1$ M (• • •). The half-wave potential ($E_{1/2}$) for the oxidation of DMFc (internal standard) was set at 0 V in each voltammogram. (b) Cyclic voltammetry of a 0.1 mM solution of [VO(salpn)] in CH_2Cl_2. Other conditions are the same as those in (a).

peak anodic and cathodic currents, respectively, E_{pa} and E_{pc} are the anodic and cathodic peak potentials, and υ is the scan rate). On the basis of these results, we can use the $DMFc^{0/+}$ couple as an internal reference to eliminate changes in $E_{Ag/AgCl}$. Figure 3b shows the voltammograms for the oxovanadium(IV/V) couple with various concentrations of the supporting electrolyte ($C^*_{PF_6^-}$), in which the average of the anodic and cathodic peak potentials (($E_{pa} + E_{pc}$)/2) for DMFc was set at 0 V. The peak potential due to the $[VO(salen)]^{0/+}$ couple is essentially independent of $C^*_{PF_6^-}$, though an additional small peak appears at very large $C^*_{PF_6^-}$, probably due to the impurity of the electrolyte.

Parts a and b of Figure 4 show cyclic voltammograms of 0.1 mM [VO(salen)] and 0.1 mM [VO(salpn)], respectively, using a microelectrode as the working electrode. The potentials are shown versus the half-wave potential ($E_{1/2}$) for the oxidation of DMFc which was also added as the internal reference. Due to the reduced *iR* drop, almost Nernstian-shaped waves are obtained even without the supporting electrolyte. The half-wave potential for the oxidation of [VO(salen)] in the absence of the supporting electrolyte (solid curve) is 0.70 V vs DMFc (Figure 4a), which is essentially unaffected by the presence of 0.1 M [NBu_4][PF_6] (dotted curve), indicating that PF_6^- does not take part in the oxidation of [VO(salen)]. On the other hand,

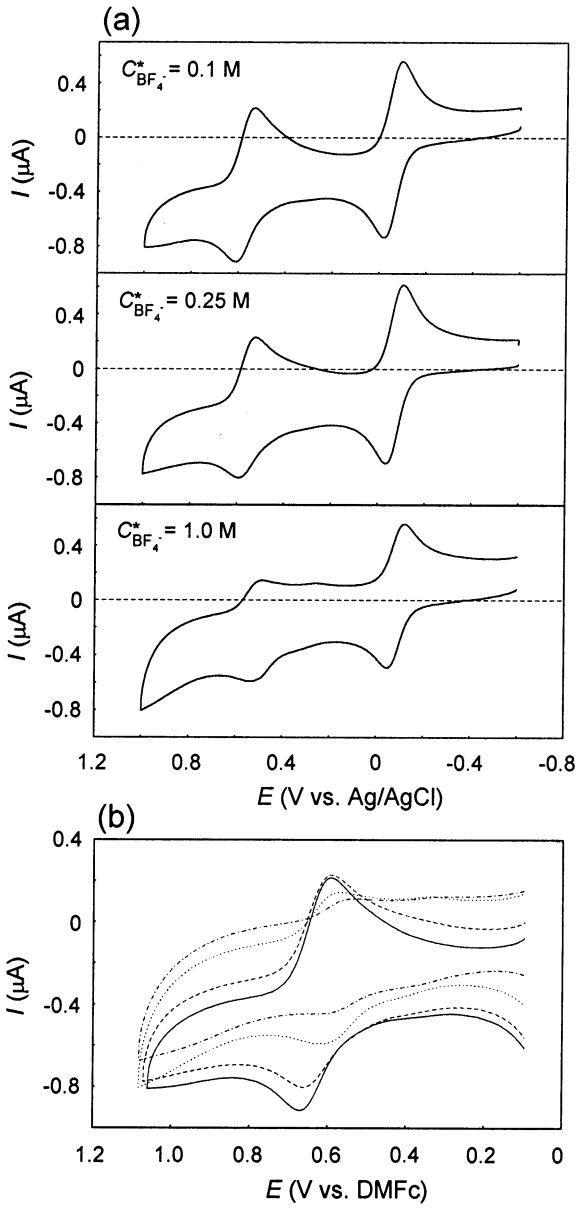

Figure 5. (a) Cyclic voltammetry of a 0.1 mM solution of [VO(salen)] in CH_2Cl_2, also containing 0.1 mM DMFc and a supporting electrolyte ([NBu_4][BF_4], $C^*_{BF_4^-} = 0.1$, 0.25, and 1.0 M). Other conditions are the same as those in Figure 3. (b) Cyclic voltammograms obtained with $C^*_{BF_4^-} = 0.1$ (—), 0.25 (– – –), 1.0 (• • •), and 2.0 M (– • –) superimposed upon each other. The average of anodic and cathodic peak potentials (($E_{pa} + E_{pc}$)/2) for DMFc was set at 0 V in each voltammogram.

the value of $E_{1/2}$ shifts to more negative values when 0.1 M [NBu_4][BF_4] is used as the supporting electrolyte (dashed curve), indicating that $[VO(salen)]^+$ is consumed in a following reaction with BF_4^- at the electrode surface. Cyclic voltammetry of [VO(salpn)] in CH_2Cl_2 in the absence of the supporting electrolyte shows an oxidation wave at $E_{1/2} =$ 0.74 V vs DMFc (Figure 4b) which is higher than that of [VO(salen)] by 0.04 V. In a similar way to [VO(salen)], the value of $E_{1/2}$ for [VO(salpn)] is essentially unaffected by the presence of 0.1 M [NBu_4][PF_6] but shifts to more negative values when 0.1 M [NBu_4][BF_4] is used as the supporting electrolyte.

Figure 5a shows cyclic voltammograms obtained with the disk electrode for solutions of 0.1 mM [VO(salen)] in the

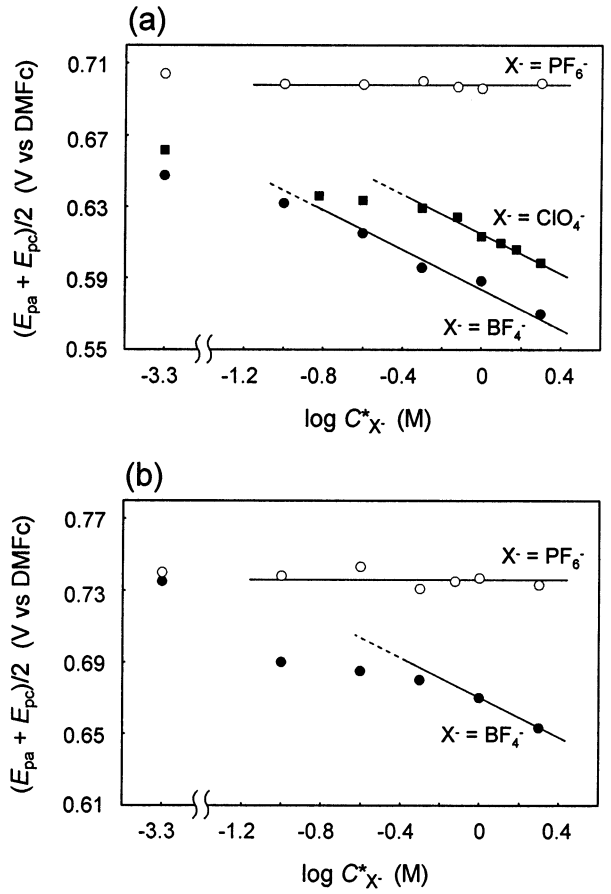

Figure 6. Dependence of the average of anodic and cathodic peak potentials ($(E_{pa} + E_{pc})/2$) for the oxovanadium(IV/V) response from (a) [VO(salen)] and (b) [VO(salpn)] on the concentration of supporting electrolyte [NBu_4][X] ($C^*_{X^-}$). The potentials are shown versus $(E_{pa} + E_{pc})/2$ for DMFc in each voltammogram.

presence of 0.1 mM DMFc and various concentrations ($C^*_{BF_4^-}$) of [NBu_4][BF_4] as the internal reference and the supporting electrolyte, respectively. Figure 5b shows the oxidation−reduction wave for the oxovanadium(IV/V) couple after the potential is standardized using the internal reference so that $E_{DMFc} = 0$ V. The average of the anodic and cathodic peak potentials ($(E_{pa} + E_{pc})/2$) for the oxovanadium(IV/V) couple shifts to more negative values as $C^*_{BF_4^-}$ increases. The peaks become less prominent at very large $C^*_{BF_4^-}$, due probably to the increased viscosity of the electrolyte solution. In the presence of a sufficient amount of [NBu_4][BF_4] ($C^*_{BF_4^-} > 0.5$ M), the potential shift for [VO(salen)] amounts to about 56 mV per decadic change in the concentration of BF_4^- (closed circles in Figure 6a), indicating that a Nernstian electron-transfer reaction (1) is coupled to a homogeneous reaction (2) which is fast enough to be considered in thermodynamic equilibrium

$$[LV^{IV}O] \rightleftharpoons [LV^{V}O]^+ + e^- \quad (1)$$

$$[LV^{V}O]^+ + BF_4^- \rightleftharpoons [LV^{V}OBF_4] \quad (2)$$

$$C_{[LV^{V}O]^+} C_{BF_4^-} / C_{[LV^{V}OBF_4]} = K_L \quad (3)$$

where L is the tetradentate Shiff-base ligand. Assuming that

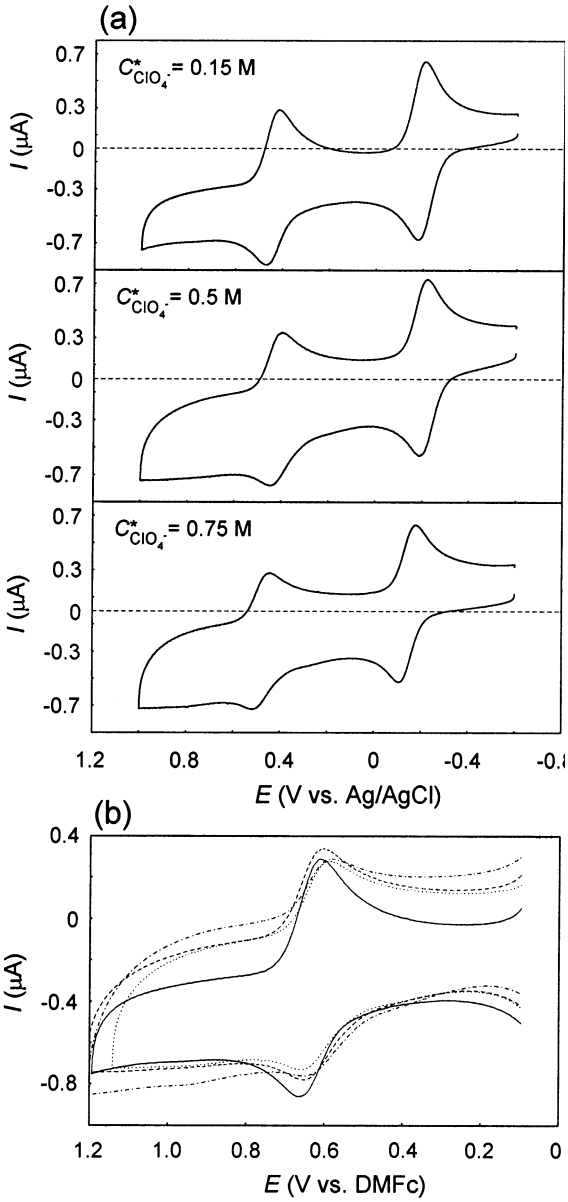

Figure 7. (a) Cyclic voltammetry of a 0.1 mM solution of [VO(salen)] in CH_2Cl_2, also containing 0.1 mM DMFc and a supporting electrolyte ([NBu_4][ClO_4], $C^*_{ClO_4^-} = 0.15$, 0.5, and 0.75 M). Other conditions are the same as those in Figure 3. (b) Cyclic voltammograms obtained with $C^*_{ClO_4^-} = 0.15$ (—), 0.5 (− − −), 0.75 (·····), and 1.0 M (—·—) superimposed upon each other. The average of anodic and cathodic peak potentials ($(E_{pa} + E_{pc})/2$) for DMFc was set at 0 V in each voltammogram.

the bulk concentration of BF_4^- ($C^*_{BF_4^-}$) is so large compared to the concentration of [$LV^{V}OBF_4$] that $C_{BF_4^-} = C^*_{BF_4^-}$ and that $K_L \ll 1$, a current−potential response in Figure 4 conforms to

$$E = E_{1/2} + 0.059 \log\{(i_l - i)/i\} \quad (4)$$

$$E_{1/2} = E^{0'} + 0.059 \log \frac{m_{[LV^{IV}O]}}{m_{[LV^{V}OBF_4]}} + 0.059 \log K_L - 0.059 \log C^*_{BF_4^-} \quad (5)$$

where i_l is a limiting current. Thus the $i-E$ curve has the usual Nernstian shape, but the half-wave potential ($E_{1/2}$) is

shifted in a negative direction ($K \ll 1$) from the position ($E^{0\prime}$) which is found for reaction (1) unperturbed by the homogeneous equilibrium (2). The magnitude of the potential shift associated with the change of $C^*_{BF_4^-}$ is so small that it is difficult to evaluate $E_{1/2}$ precisely from the voltammogram obtained with the microelectrode. A more reliable numerical value, $(E_{pa} + E_{pc})/2$ obtained with the disk electrode, can be used to represent the redox potential of the oxovanadium(IV/V) couple. On the basis of the lack of interaction between PF_6^- and $[VO(salen)]^+$, the mean value of $(E_{pa} + E_{pc})/2$ obtained with $[NBu_4][PF_6]$ (open circles in Figure 6a) provides $E^{0\prime} = 0.698$ V for [VO(salen)]. Similarly, the value of $E^{0\prime}$ for [VO(salpn)] is evaluated to be 0.737 V from Figure 6b. Because the difference between the mass transfer coefficients $m_{[LV^{IV}O]}$ and $m_{[LV^{V}OBF_4]}$ may be disregarded, an equilibrium constant of $K_{salen} = 9.0 \times 10^{-3}$ M is calculated from the potential shift of $E_{1/2} - E^{0\prime} = -0.103$ V for [VO(salen)] caused by the presence of 0.5 M $[NBu_4][BF_4]$, which is comparable with that evaluated by NMR. Analogous experiments for [VO(salpn)] yield the potential shift of $E_{1/2} - E^{0\prime} = -0.067$ V caused by the presence of 1 M $[NBu_4][BF_4]$ (Figure 6b) and a larger dissociation constant of $K_{salpn} = 7.3 \times 10^{-2}$ M. Thus, the affinity of $[VO(salpn)]^+$ for BF_4^- as an axial ligand is much smaller than that of $[VO(salen)]^+$. A weak coordination of ClO_4^- to $[VO(salen)]^+$ is also evidenced by the dependence of $(E_{pa} + E_{pc})/2$ on $C^*_{ClO_4^-}$. The potential shifts are very small (closed squares in Figure 6a) but could be determined from the voltammograms (Figure 7) using DMFc as the internal standard. The dissociation constant for the coordination of ClO_4^- to $[VO(salen)]^+$ is evaluated to be 3.3×10^{-2} M.

The coordination of these electrolyte anions to oxovanadium(V) complexes is so weak that it can easily be overshadowed by the presence of other ligands such as polar solvent molecules. Indeed, the redox potential for the oxovanadium(IV/V) couple in CH_3CN is independent of $C^*_{BF_4^-}$, indicating that the coordination of CH_3CN is favored over that of BF_4^-.

Conclusions

The weak coordination of BF_4^- to oxovanadium(V) complexes governed by formation constants of $K^{-1} \sim 10^2$ M^{-1} in CH_2Cl_2 is demonstrated in this study. The coordination of BF_4^- to oxovanadium(V) complexes may have been overlooked in the previous studies because it is evasive even in CH_2Cl_2 due to the very small K_L^{-1} values. The potential shift according to eq 5 is detectable only in the presence of a large amount of BF_4^- and with the use of the internal reference to compensate for changes in junction potentials. The results may provide a useful information to reevaluate a large number of previous results on the electrochemistry of oxovanadium(IV and V) complexes in the presence of BF_4^- as the electrolyte.

Acknowledgment. We thank Prof. Fred C. Anson for helpful discussions. We also thank Prof. Kohtaro Osakada for discussions in X-ray crystallography. This work was partially supported by a Grant-in-Aid for Scientific Research (No. 14703029) from MEXT, Japan.

Supporting Information Available: Tables giving atomic coordinates, equivalent isotropic thermal parameters, and anisotropic displacement parameters for $[VO(salen)BF_4]$ and $[VO(salpn)NCCH_3][BF_4]$. This material is available free of charge via the Internet at http://pubs.acs.org.

IC0205987